Quantum-to-classical transition in a system with mixed classical dynamics

Fabricio Toscano
Fundação Centro de Ciências e Educação Superior a Distância do Estado do Rio de Janeiro, 20943-001 Rio de Janeiro, RJ, Brazil and Instituto de Física, Universidade Federal do Rio de Janeiro, Cx. P. 68528, 21941-972 Rio de Janeiro, RJ, Brazil

Diego A. Wisniacki
Departamento de Física "J. J. Giambiagi," FCEN, UBA, 1428 Buenos Aires, Argentina
(Received 2 June 2006; published 27 November 2006)

We study how decoherence rules the quantum-classical transition of the kicked harmonic oscillator. The system presents classical dynamics that ranges from regular to strong chaotic behavior depending on the amplitude of the kicks. We show that for regular and mixed classical dynamics, and in the presence of noise, the distance between the classical and quantum phase space distributions is proportional to a single parameter $\chi \equiv K\hbar_{\mathrm{eff}}^2/4D^{3/2}$, which relates the effective Planck constant, $\hbar_{\mathrm{eff}}$, to the kicking strength, K, and the diffusion constant, D. This relation between classical and quantum distributions is valid when $\chi < 1$, a case that is always attainable in the semiclassical regime, independent of the value of the strength of noise given by D. Our results extend a recent study performed in the chaotic regime.

DOI: 10.1103/PhysRevE.74.056208 PACS number(s): 05.45.−a, 03.65.Ta

I. INTRODUCTION

A fundamental problem that has attracted substantial attention since the beginning of quantum mechanics is the complete description of the emergence of the classical world within the quantum theory. In spite of many advances achieved in the field, a number of questions remain unanswered. Within the milestones in this field, we can cite the understanding that the formalism of phase space distribution functions is the appropriate framework to study the quantum to classical transition [1]. In this regard, the Wigner function [2] has the advantage, among all quantum phase-space distributions, that it identifies the nonlinearities of the system as responsible for the separation between the quantum and the classical evolution. Moreover, while the Wigner distribution obeys the Liouville equation of the classical distribution for linear systems, the nonlinearities add terms to this equation that eventually set the two distributions apart [3] even for initial states that are classically allowed.

The time for which classical and quantum distributions start to differ (known as breaking or separation time) can be very short for classically chaotic systems. This is the consequence of nonlinearities of the system being reached very quickly due to the exponential stretching of the distributions. Therefore, the breaking time scales as $\ln(1/\hbar_{\mathrm{eff}})$, where the effective Planck constant $\hbar_{\mathrm{eff}} \equiv \hbar/S$ is the semiclassical parameter (with S a typical action of the system) [4–10].

Furthermore, an important and subtle problem is that, due to its logarithmic behavior, the separation time for macroscopic systems ($\hbar_{\mathrm{eff}} \ll 1$) can still be small in comparison to a typical evolution time allowing quantum effects that are not observed in the classical world [11]. This paradoxical situation is explained by the coupling of the system with the environment leading to the elimination of the quantum signatures providing reconciliation of theory and observation [12,13]. Furthermore, it is unclear how the effects of the environment affect the logarithmic law of the breaking time in systems with a classical chaotic dynamics. More precisely, the exact relation between the strength of noise and the effective Planck constant in order to obtain the correct classical limit is still unknown [14].

Answers to these problems can be found in a recent work [15] where the authors studied the effect of a purely diffusive environment over a specific model given by the kicked harmonic oscillator (KHO). In that paper, it is shown that the differences between the classical and quantum phase evolution are proportional to a single parameter $\chi = K\hbar_{\mathrm{eff}}^2/4D^{3/2}$. This parameter χ combines $\hbar_{\mathrm{eff}}$, the diffusion coefficient D, and the kicking strength K, which controls the macroscopicity, the noise, and the chaotic behavior, respectively. These quantum-classical differences were estimated with $\mathcal{D}_n$ (n is the number of kicks), which is the integral over the whole phase space of the modulus of the difference between the quantum and the classical distributions. Thus, the authors showed that when the classical dynamic is chaotic in the semiclassical limit, $\hbar_{\mathrm{eff}} \ll 1$, and when $\chi < 1$, the single parameter χ controls the quantum-classical transition of the KHO. These results confirm the conjecture presented in Ref. [16] that, in the presence of noise a single parameter controls the quantum-classical transition of classically chaotic systems.

In this paper we analyze the case when the classical dynamics of the KHO is regular or mixed. We show that the separation between the quantum and the classical evolution can be characterized through the behavior of $\mathcal{D}_n$ as a function of time in the absence of a reservoir. When the initial distribution explores regions of regular classical dynamics, the behavior of $\mathcal{D}_n$ allows the identification of a power law, $1/\hbar_{\mathrm{eff}}^{\alpha}$, for the separation time. However, this scale-law is not valid when the degree of mixing increases. In the presence of a purely diffusive reservoir, we show that the quantum-classical differences measured by $\mathcal{D}_n$ also scale with the parameter χ in the semiclassical limit and when $\chi < 1$. Hence, the concept of separation time is not meaningful any more because the quantum and the classical distributions remain close throughout the evolution. Our result suggests that the

conjecture introduced in Ref. [16] can be extended independently of the underlying classical dynamics.

The paper is organized as follows. Section II is focused on reviewing the quantum and the classical versions of the KHO and explaining the formalism for the evolution of the Wigner function and the classical distribution as a map in phase space. In Sec. III we introduce our measure of the quantum-classical differences, $\mathcal{D}_n$, and study its behavior as a function of time without the presence of a reservoir. We also investigate the scale-law with the effective Planck constant of the separation time when the initial distribution explores regular or mixed regions of the phase space. The effects of decoherence over $\mathcal{D}_n$ when the KHO is in contact with a purely diffusive reservoir are studied in Sec. IV. Finally, we include some final remarks in Sec. V.

II. MODEL: THE KICKED HARMONIC OSCILLATOR

A. The quantum version

The model used in our calculations is KHO, a particle of mass, m, in a harmonic potential subject to a periodically applied position-dependent delta pulses. The quantum Hamiltonian is defined as

$$\hat{H} = \frac{\hat{P}^2}{2m} + \frac{1}{2}m\nu^2\hat{Q}^2 + A\cos(k\hat{Q})\sum_{n=0}^{\infty}\delta(t-n\tau), \qquad (1)$$

where ν is the oscillator frequency, A the amplitude of the kicks, and τ the interval between two consecutive kicks. The periodicity of the position dependent kicking potential is set by k.

The physical realization of this Hamiltonian is within the context of trapped ions. It was shown in Ref. [17] that it describes the center-of-mass dynamics of an ion in a one-dimensional trap submitted to a sequence of standing-wave laser pulses, off-resonance with a transition between the electronic ground state and another internal state. The wave number k in Eq. (1) is the projection along the trap axis of the corresponding wave vectors with equal modulus $|\vec{k}|$ of two opposite propagating pulses with oblique incidence measured by an angle θ, i.e., $k \equiv 2|\vec{k}|\cos(\theta)$.

Working with dimensionless quantities $\hat{q}=k\hat{Q}$, $\hat{p}=k\hat{P}/m\nu$, and $K=k^2A/m\nu$, it is possible to define an effective Planck constant $\hbar_{\text{eff}}$, so that $[\hat{q},\hat{p}]=2i\eta^2 \equiv i\hbar_{\text{eff}}$, with $\eta=k\Delta Q_0 = k\sqrt{\hbar/2m\nu}$ and ΔQ_0 being the width of the ground state of the harmonic oscillator. The dimensionless parameter η is the so-called Lamb-Dicke parameter [18], which measures the ratio between the ground state width and the wavelength $\lambda=2\pi/k$ (the scale of the nonlinearity of the Hamiltonian). In experiments with trapped ions, the classical limit $\eta \to 0$ (and thus $\hbar_{\text{eff}} \equiv 2\eta^2 \to 0$) can be approximated simply by changing the angle θ of incidence of the incoming pulses or by increasing the trap frequency ν.

B. The classical version

The classical Hamiltonian is obtained from Eq. (1) by replacing the quantum operators $\hat{Q}$ and $\hat{P}$ by the phase space variables Q and P, respectively. In an analogous way, we can define the dimensionless phase space coordinates $\mathbf{x} \equiv (q,p) \equiv (kQ, kP/m\nu)$. Then, the time-dependent classical evolution can be described as a composition of a discrete map corresponding to the kick, plus a rotation in phase space, $\mathbf{x}_{n+1} = \mathbf{R} \circ \mathbf{K}(\mathbf{x}_n)$, where $\mathbf{x}_n \equiv (q_n, p_n)$ are the coordinates before kick n (where the first kick corresponds to $n=0$). The kick operation $\mathbf{K}$ is defined as

$$q_n^+ = q_n, \quad p_n^+ = p_n + K\sin(q_n), \qquad (2)$$

and the phase space rotation $\mathbf{R}$ is given by

$$q_{n+1} = \cos(\nu\tau)q_n^+ + \sin(\nu\tau)p_n^+,$$

$$p_{n+1} = -\sin(\nu\tau)q_n^+ + \cos(\nu\tau)p_n^+. \qquad (3)$$

In close relation with Ref. [15], we have also considered the case where the interval between kicks τ and the period of the harmonic oscillator $T=2\pi/\nu$ are related by $\tau=T/6$.

The phase space of the system is unbounded and corresponds to a mixed dynamics exhibiting stable islands surrounded by a stochastic web. The thickness of the web is controlled by the dimensionless kick amplitude, $K=k^2A/m\nu$. Hence, these chaotic regions broaden (shrink) as K increases (decreases). In the considered case of $\tau=T/6$, the stochastic web displays crystal hexagonal symmetry [7,9]. In Fig. 1 we show the stroboscopic phase space around the origin for different values of K. For $K \leqslant K_c \approx 1.1547$, the origin is an elliptic fixed point while for $K > K_c$ the system undergoes a bifurcation where the origin becomes an hyperbolic fixed point and two neighbor elliptic fixed points arise. The separation between these two elliptic fixed points increases with K. As we can see in Fig. 1(a), for $K=0.5$ the dynamics of the system around the origin is essentially regular with a series

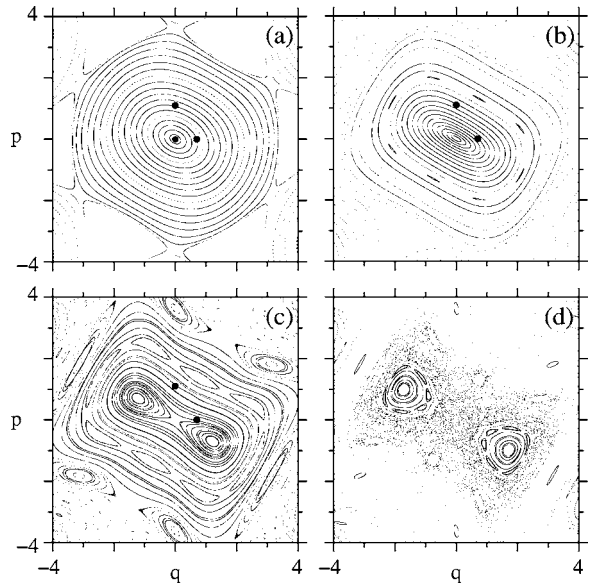

FIG. 1. Stroboscopic phase space of the KHO for different values of the kick amplitude K. In (a) $K=0.5$, (b) $K=1.0$, (c) $K=1.5$, and in (d) $K=2.0$. The phase space points $(q_0,p_0)=(0,0)$, (0,1.1), and (0.7,0), marked with symbols (●), are the centers of the initial coherent states used in our numerical simulations.

of concentric tori around the elliptic fixed point. For $K=1$ [Fig. 1(b)], some tori were destroyed and tiny chaotic regions appear (invisible to the eye). Mixed dynamics start to manifest most appreciably for $K=1.5$ while for $K=2$ most of the area around the origin shows chaotic behavior [see Figs. 1(c) and 1(d)].

C. The evolution of phase space distributions without reservoir

We analyze the quantum-classical transition in phase space comparing the evolution of the Wigner function [2] and the corresponding classical distribution. The Wigner function is defined as

$$W(\mathbf{x}) \equiv \int dy \left\langle q + y/2 \left| \frac{\hat{\rho}}{4\pi\eta^2} \right| q - y/2 \right\rangle \exp\left\{ -i\frac{py}{2\eta^2} \right\}, \tag{4}$$

with $\hat{\rho}$ the density operator of the quantum state. This quantum phase space distribution is advantageous, because it is the only one to yield the correct marginal probabilities, thus satisfying an important property of classical distributions [19]. Furthermore, quantum effects are more pronounced as compared to other bounded distributions. Finally, new methods have been developed for the direct measurement of the Wigner function, which are adequate for the description of evolving systems [20,21].

Without the action of a reservoir, the unitary evolution of the Wigner function of the KHO can be written as [5,15]

$$W_{n+1}(\mathbf{x}) = \int d\mathbf{x}' L(\mathbf{x}^R, \mathbf{x}') W_n(\mathbf{x}'), \tag{5}$$

where W_{n+1} and W_n are the Wigner functions immediately before the kicks $n+1$ and n, respectively. The integration is over all the unbounded phase space and

$$L(\mathbf{x}^R, \mathbf{x}') \equiv \int_{-\infty}^{\infty} \frac{d\mu}{2\pi\eta^2} e^{i/\eta^2 [K \sin(q')\sin(\mu) - \mu(p^R - p')]} \delta(q^R - q') \tag{6}$$

is the quantum propagator of one kick plus the harmonic evolution between the consecutive kicks which is given by

$$\mathbf{x}^R \equiv [q^R(\mathbf{x}), p^R(\mathbf{x})] \equiv \mathbf{R}^{-1}(\mathbf{x}), \tag{7}$$

i.e., the phase space coordinates rotated with the inverse transformation of Eq. (3). The Liouville evolution of the classical distribution, $W_n^{\mathrm{cl}}(\mathbf{x})$, can also be written in the form of Eq. (5) with the classical propagator

$$L^{\mathrm{cl}}(\mathbf{x}^R, \mathbf{x}') \equiv \delta[p' - p^R + K \sin(q')] \delta(q^R - q'). \tag{8}$$

In the classical limit $\eta \to 0$, the classical propagator is formally recovered from the quantum one [5]. Indeed, in the semiclassical regime ($\eta \ll 1$), the integral in Eq. (6) can be estimated by employing stationary-phase techniques yielding

$$L(\mathbf{x}^R, \mathbf{x}') \approx \frac{1}{|b|^{1/3}} \mathrm{Ai}\left(-\frac{\mathrm{sign}(b)}{|b|^{1/3}} (p' - p^R + K \sin(q')) \right) \times \delta(q^R - q'), \tag{9}$$

where $b = (\eta^4 K/2)\sin(q')$ and $\mathrm{Ai}(x)$ is the Airy function. When $\eta \to 0$, we can use $\mathrm{Ai}\{-y/\varepsilon\}/\varepsilon \overset{\varepsilon \to 0}{\to} \delta(y)$ to get the classical Liouville propagator in Eq. (8). However, no matter how small we can do the Lamb-Dicke parameter, η, in a physical realization of the KHO, this will always take a finite value and then the presence of an Airy function in the quantum propagator will eventually set the Wigner function and the classical distribution apart.

III. THE QUANTUM-CLASSICAL SEPARATION WITHOUT RESERVOIR: SCALE-LAW FOR THE SEPARATION TIME

The Wigner distribution of a linear system (quadratic Hamiltonian) satisfies the Liouville equation for the classical phase-space probability distribution. Thus, starting with a Wigner function of a pure state that corresponds to a classically allowed probability distribution (the only possibility is a minimum uncertainty initial Gaussian wave packet [22]), a linear dynamics evolution will preserve its Gaussian shape. The initial wave packet will deform and eventually delocalize during the evolution when the system has nonlinearities. As a consequence, quantum interference effects appear between different pieces of the wave packet which remain coherent throughout the unitary evolution. These quantum interference effects stem from the extra terms that the nonlinearities of the system add to the Liouville equation in order to obtain the correct equation of motion of the Wigner function [3,23]. Similarly, these interferences are originated by the nonlocal nature of the Wigner propagator [see, for example, Eq. (6) in comparison with the local nature of the Liouville propagator of Eq. (8)], that persist even in the semiclassical regime [see Eq. (9)]. Therefore, interference effects are responsible for the separation of the Wigner function from the classical distribution and, thus, of the quantum-classical correspondence breakdown.

The quantum-classical differences start to become important when the initial distribution spreads over distances of the order of the characteristic scale of the nonlinearities of the system. This argument is used in order to estimate the time scale for the separation in the case of classically chaotic systems [11,13,24]. Indeed, as the initial Gaussian Wigner function is well localized, it will initially evolve following classical trajectories in phase space. The wave packet will stretch exponentially fast along the unstable manifold and will also shrink exponentially fast along the stable one in order to conserve the phase space volume. This is followed by the characteristic folding of classical trajectories that forces the wave packet to develop quantum interference between different pieces that are coherently related. As a consequence of this behavior, a logarithmic scale law with the effective Planck constant $\hbar_{\mathrm{eff}}$ of the separation time in systems with classical chaotic dynamics is found. For the KHO, the separation time t_s results

$$t_s = n_s \tau \approx \frac{\tau}{\Lambda} \ln(1/\eta), \tag{10}$$

where Λ is the local expansion coefficient and $\hbar_{\text{eff}}=2\eta^2$. A detailed estimation of t_s can be found in Refs. [7,10] and in Ref. [9] where is also shown a numerical test that indicates that this is also the time when quantum and classical expectation values start to differ from each other. The expansion coefficient Λ corresponds to the Lyapunov exponent when an average over initial conditions in the chaotic regions is considered [10,15].

Conversely, when the classical dynamics of the system is essentially regular, the scaling law of the quantum-classical separation time with $\hbar_{\text{eff}}$ has been less studied. The logarithmic dependence of t_s in the chaotic case is due to the exponential divergence of classical trajectories, but in the integrable case, the divergence is typically polynomial [13,25,26]. Therefore, following a similar type of argument as in the chaotic case, the separation time in regular systems would follow a power law. If the initial distribution explores regions of essentially regular dynamics in the KHO, we would have

$$t_s = n_s \tau \approx \tau/\eta^{\alpha}, \tag{11}$$

where we do not include the numerical constants. Indications of the validity of Eq. (11) for $K \ll 1$ are given in Ref. [7]. In the following we will show a way to estimate the amount of quantum effects that lead to the separation between the Wigner function and the classical distribution and how the scaling law for the separation time in Eq. (11) manifests in our formalism.

In Ref. [15], the time dependent quantity ($t=n\tau$),

$$\mathcal{D}_n \equiv \int d\mathbf{x} |W_n(\mathbf{x}) - W_n^{\text{cl}}(\mathbf{x})|, \tag{12}$$

was introduced to quantify the quantum effects that lead to the separation between the Wigner function, W_n, and the classical distribution, W_n^{cl}. Starting with the same initial distribution, it is expected that during the unitary evolution the appearance of quantum-classical differences make $\mathcal{D}_n$ grow and eventually saturate around some finite value. This behavior is shown in Figs. 2 and 3 where we have plotted $\mathcal{D}_n$ as a function of the scaled number of kicks (see below) for different values of the semiclassical parameter, η, and the amplitude of the kick, K. The initial distribution is always a coherent state with width $\Delta q(0)=\Delta p(0)=\eta$.

In Fig. 2 the amplitude of the kick is $K=0.5$. This case involves regular classical dynamics because the different initial coherent states considered, during the interval of times monitored, spread over the regular region around the origin (see Figs. 1, 4, and 5). Figure 2(a) corresponds to an initial coherent state centered at the phase space point $(q0,p0)=(0,1.1)$. We can see that, as a result of starting with an initial wave packet outside the origin, the quantity $\mathcal{D}_n$ grows up to values larger than one for all values of the semiclassical parameter η. We remark that for each value of η, the quantity $\mathcal{D}_n$ saturates at a different value always larger than one (not showed in the plot). That $\mathcal{D}_n$ attains values of the order $\mathcal{O}(1)$ clearly indicates the separation between the Wigner and the classical distributions because a measure of their differences reaches values of the order of their normalization. However, it is important to note that, independent of the value of the quantum differences, we choose to define the separation between the Wigner and classical distributions, it will be reached at some early time of the evolution independently of how small is the semiclassical parameter η. Thus, the separation time defined in this way should scale as in Eq. (11). This is shown in the plots, where a rescaling of the number of kicks by a function of the form $n^*(\eta)=\eta^{-\alpha}$ allows the approximately collapse of all the curves. The difference between the values $\alpha=0.4$ and $\alpha=1.8$ in Figs. 2(a) and 2(b), respectively, come from the distinct dynamical evolution de-

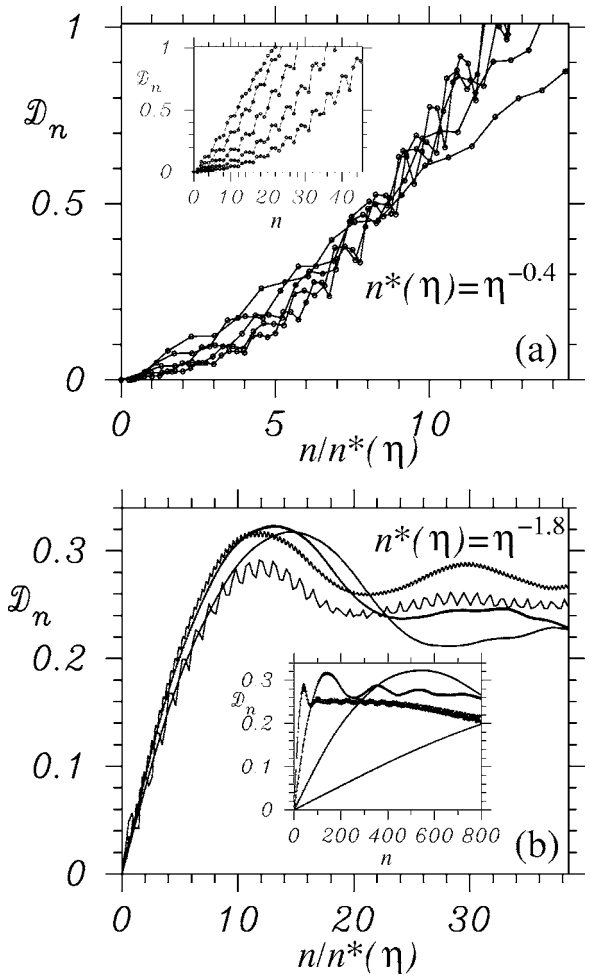

FIG. 2. Separation $\mathcal{D}_n$ between quantum and classical distribution as a function of the number of kicks for $K=0.5$. The full lines join all the values of $\mathcal{D}_n$ calculated for the same value of the Lamb-Dicke parameter η. In (a) the initial distribution is a coherent state centered at the phase space point $(q0,p0)=(0,1.1)$ and the curves are for $\eta=0.5$, 0.25, 0.125, 0.0625, and 0.03125. In (b) the initial coherent state is centered at the origin and the curves are for $\eta=0.5$, 0.25, 0.125, and 0.0625. The number of kicks, n, are rescaled by a function $n^*(\eta)=\eta^{-\alpha}$, where we optimize the values of α in order to obtain the best collapsing of all the curves. The insets show the curves without the rescaling over the time n. The curves in both insets corresponds to decreasing values of η from left to right.

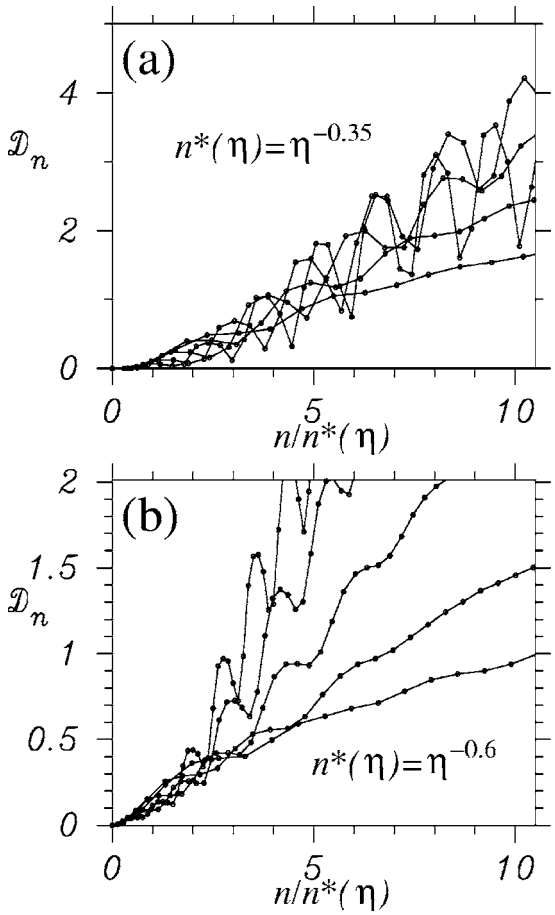

FIG. 3. Same as Fig. 2 but for $K=1.0$. In (a) the initial coherent state centered at $(q0,p0)=(0,1.1)$ and in (b) $(q0,p0)=(0.7,0)$. The different curves in each plot correspond to $\eta=0.5$, 0.25, 0.125, 0.0625, and 0.03125. The number of kicks, n, is rescaled by a function $n^*(\eta)=\eta^{-\alpha}$ where we optimize the values of α in order to obtain the best collapsing of all the curves.

veloped from the initial wave packets. In the first case, the initial wave packet is centered outside the origin and the distribution move around a torus and it is stretching around it. Conversely, in the case of Fig. 2(b) the center of the wave packet is at rest because the origin is a fixed point of the classical map. We have found $\alpha=0.75$ when the initial distribution is centered at $(q_0,p_0)=(0.7,0)$. This case is similar to Fig. 2(a) so we do not show it here. Hence, we see that the value of α in the separation time $n_s(\eta)\approx\eta^{-\alpha}$ will depend on the local dynamics explored by the initial distribution. This is similar to what happens to the separation time, $n_s(\eta)\approx(1/\Lambda)\ln(1/\eta)$, in the chaotic regime where the value of Λ reflects the character of the local dynamics explored by the initial distribution.

In Fig. 2(b) we show the case when the initial coherent state is centered at the origin of phase space when $K=0.5$. $\mathcal{D}_n$ grows up to values around 0.25 and then saturates for all semiclassical parameters η. In this case, $\mathcal{D}_n$ grow less than when the initial coherent state is outside the origin because now the quantum and classical distributions remain well localized for very long times and, thus, the quantum-classical differences are less pronounced (Fig. 5). Nevertheless, these differences do not decrease for small values of η showing that the separation between classical and quantum evolution occurs in the semiclassical regime. The fluctuations observed in Figs. 2(a) and 2(b) have a period of $n\approx 6$ kicks, i.e., approximately the period of the harmonic evolution $T=6\tau$. This is the time that most parts of the quantum and classical distribution take to complete a spin along the elliptical structure of phase space around the origin for $K=0.5$ (see Fig. 1). Furthermore, it is interested to compare in Figs. 4 and 5 the quantum-classical differences that lead to the separation between the quantum and the classical evolution when the amplitude of the kick is $K=0.5$. Indeed, when the initial coherent state is centered outside the origin, the quantum and classical distributions spread out and, as a consequence, the Wigner function develops a quantum interference pattern throughout the evolution. This clearly indicates its separation from the classical distribution (see Fig. 4). When the initial coherent state is centered at the origin of phase space, which is an elliptical fixed point for $K=0.5$, the quantum and the classical distributions remain well localized for very long times (Fig. 5). In this case, the classical distribution develops the typical classical structure of "whorls" associated with an elliptic fixed point [5,21]. It is evident from Figs. 4 and 5 that the quantum evolution smoothes out this detail of the classical distribution and this is the origin of the quantum-classical differences that lead to the separation.

Figure 3 shows the case when the kicking amplitude is $K=1$. In this situation, all the initial distributions considered explore the region around the phase space origin that is spread of tiny chaotic regions. It is noteworthy that in this case the collapsing of all the curves does not work well, indicating the departure of the separation time from the power law [Eq. (11)] when the degree of mixing in the classical dynamics grows. We stress that when $K=1.5$, which is a case of a great degree of mixing in the classical dynamics, it is not possible to rescale the number of kicks by a function of the form $n^*(\eta)=\eta^{-\alpha}$ in order to obtain an approximately collapse of all the curves $\mathcal{D}_n$ versus n.

IV. DECOHERENCE: THE EFFECT OF A DIFFUSIVE ENVIRONMENT

In this section we study how the decoherence affects the quantum-classical differences given by the quantity $\mathcal{D}_n$, when the initial distribution explores phase space regions of regular or mixed classical dynamics. Our approach is in line with the one developed in Ref. [15], where the case of chaotic dynamics was studied. Therefore, we also coupled the KHO to a thermal reservoir with average population $\bar{n}$, in the Markovian and weak coupling limit and considering the purely diffusive regime (the high temperature regime $\bar{n}\to\infty$ together with $\Gamma\to 0$ but when $\bar{n}\Gamma$ is constant, where Γ is the dissipation rate). In this limit, the action of the reservoir over the Wigner function is described by the Fokker-Planck equation,

$$\left.\frac{\partial W}{\partial t}\right|_{\text{reservoir}}=\tilde{\Gamma}\left(\frac{\partial^2 W}{\partial q^2}+\frac{\partial^2 W}{\partial p^2}\right), \tag{13}$$

with $\tilde{\Gamma}\equiv\bar{n}\Gamma\eta^2$. For the complete evolution we have to add to the right-hand side (RHS) of Eq. (13) the unitary evolution

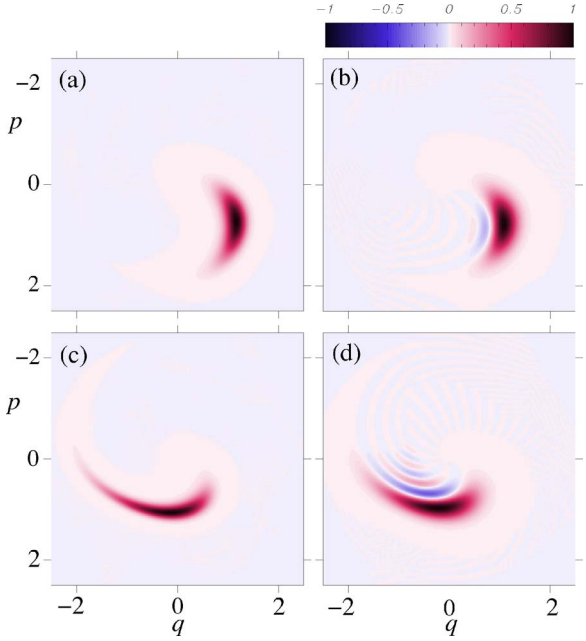

FIG. 4. (Color online) Density plots of the Wigner (right) and classical distributions (left) that result from the evolution with the KHO Hamiltonian with the kick amplitude $K=0.5$ from an initial coherent state centered in the phase space point $(q_0,p_0)=(0.0,1.1)$ and with a width $\Delta q(0)=\Delta p(0)=\eta=0.25$. In (a) and (b) immediately before the kick $n=8$ and in (c) and (d) immediately before the kick $n=18$.

given by the Hamiltonian in Eq. (1). The action of a pure diffusive reservoir over a classical distribution is also described by Eq. (13) if we identify $\tilde{\Gamma}$ with the classical diffusion constant. In this case, we must add to the RHS of Eq. (13) the corresponding Liouville term of the classical dynamics to obtain the complete evolution.

Our findings on the behavior of the quantity $\mathcal{D}_n$ in the presence of decoherence are a consequence of the effects of the reservoir over the one kick propagator of the Wigner function that brings it close to the classical propagator of one kick. Hence, we first summarize the steps in Ref. [15] that allow us to write the one kick propagator of the Wigner function as a function of the one kick propagator of the classical distribution under the action of a purely diffusive reservoir and in the semiclassical regime ($\eta \ll 1$).

The solution of the differential equations for the evolutions of both, the classical and the quantum distributions, in the interval of time between two consecutive kicks, and in the presence of the purely diffusive reservoir, can be written as in Eq. (5) where we have to replace the one kick propagator $L(\bar{\mathbf{x}},\mathbf{x}')$ of Eqs. (6) and (8) by the smoothed one,

$$\tilde{L}(\mathbf{x}^R,\mathbf{x}') \equiv \int \frac{d\bar{\mathbf{x}}}{4\pi D} L(\bar{\mathbf{x}},\mathbf{x}') \exp\left(-\frac{(\bar{\mathbf{x}}-\mathbf{x}^R)^2}{4D}\right). \quad (14)$$

Here, $D=\tilde{\Gamma}\tau$ is the diffusion constant between two consecutive kicks, and $\mathbf{x}^R$ is the result of the harmonic evolution given in Eq. (7). Then, the classical smoothed propagator for the classical distribution function is

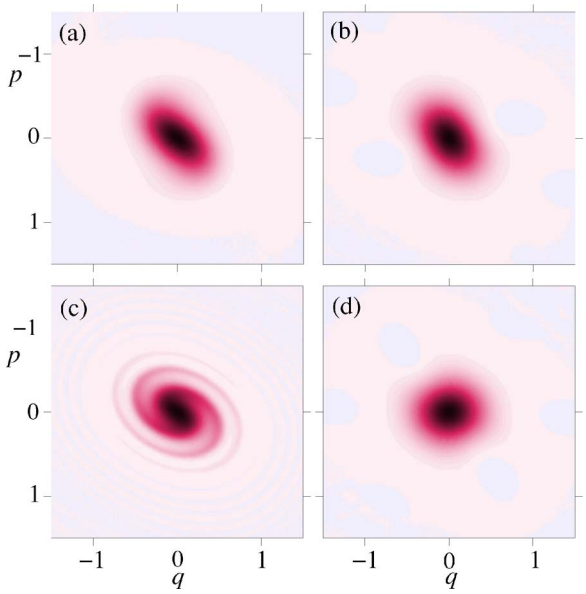

FIG. 5. (Color online) Density plots of the Wigner (right) and classical distributions (left) that result from the evolution with the KHO Hamiltonian with the kick amplitude $K=0.5$ from an initial coherent state centered at the origin of phase space and with a width $\Delta q(0)=\Delta p(0)=\eta=0.25$. In (a) and (b) immediately before the kick $n=60$ and in (c) and (d) immediately before the kick $n=300$.

$$\tilde{L}^{\mathrm{cl}}(\mathbf{x}^R,\mathbf{x}') = \frac{e^{-(x^2+y^2)}}{4\pi D}, \quad (15)$$

where $y=(p'-p^R+K\sin q')/2\sqrt{D}$ and $x=(q'-q^R)/2\sqrt{D}$. In the same way, we performed the integration in Eq. (14) over the propagator in Eq. (6) to obtain the smoothed quantum propagator:

$$\tilde{L}(\mathbf{x}^R,\mathbf{x}') \equiv \int_{-\infty}^{+\infty} \frac{d\mu}{2\pi\eta^2} e^{-D\mu^2/\eta^4} e^{i/\eta^2[K\sin(q')\sin(\mu)-\mu(p^R-p')]} \times \delta(q^R-q'). \quad (16)$$

The presence of the Gaussian factor $\exp(-D\mu^2/\eta^4)$ in the integrand allows us to obtain an approximation in terms of the classical smoothed propagator given by Eq. (15). Indeed, when the width of this Gaussian is small, $\eta^2/\sqrt{D} \ll 1$, the μ' that effectively contribute to the integration are those close to the origin. Therefore, we can use $\sin(\mu)\approx\mu-\mu^3/6$ in the phase of the integrand. Moreover, if $\chi=K\eta^4/D^{3/2} \ll 1$, the term with μ^3 in the phase is small, so we can also approximate $e^{i(\theta+\delta)}\approx e^{i\theta}+i\delta e^{i\theta}$ and then the μ-integration can be performed. Thus, we obtain the following approximation to the smoothed quantum propagator

$$\tilde{L}(\mathbf{x}^R,\mathbf{x}') \approx \tilde{L}^{\mathrm{cl}}(\mathbf{x}^R,\mathbf{x}')[1+\chi\sin(q')f(y)], \quad (17)$$

where $f(y)=1/4(y-2y^3/3)$. Since $|f(y)\exp(-y^2)| \leq 0.081$, Eq. (17) is valid under the less restrictive condition $\chi \lesssim 1$. It is important to note that the smoothed quantum propagator [Eq. (17)] is obtained without any assumption of the underlying classical dynamics of the system. The only conditions that have to be fulfilled are: (i) $D \gg \eta^4$ and (ii) $D \gtrsim (K\eta^4)^{2/3}$.

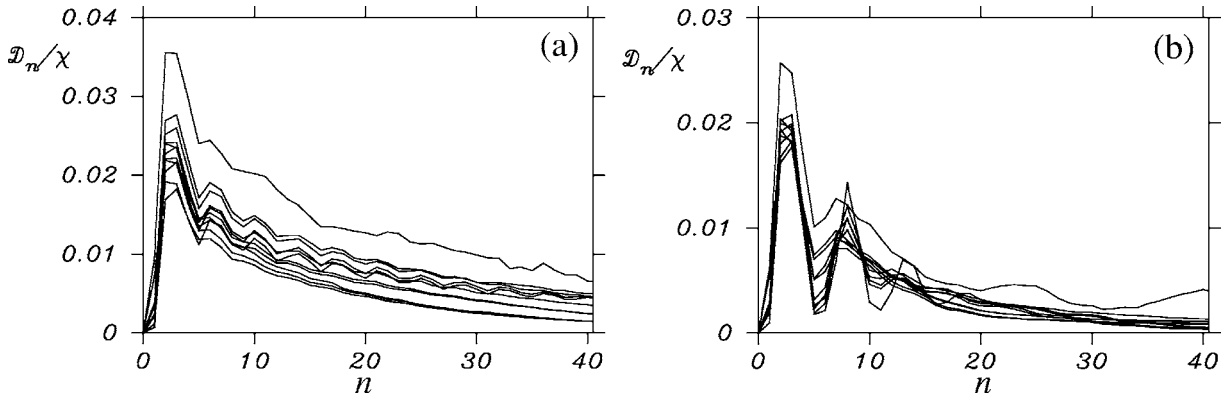

FIG. 6. Renormalized distances between quantum and classical distributions, with diffusion. All the curves were generated with the initial coherent state centered in the phase-space point $(q_0,p_0)=(0,1.1)$ (see Fig. 1) with the kick amplitude $K=0.5$ in (a) and $K=1.5$ in (b). The eleven different curves correspond to $\chi \equiv K\eta^4/D^{3/2}=6.2\times10^{-2},4.3\times10^{-2},1.5\times10^{-2},1.1\times10^{-2},7.6\times10^{-3},3.9\times10^{-3},1.4\times10^{-3},6.8\times10^{-4},4.8\times10^{-4},2.4\times10^{-4},4.3\times10^{-5}$ in (a) and $\chi=6.5\times10^{-2},4.5\times10^{-2},3.3\times10^{-2},2.3\times10^{-2},1.2\times10^{-2},4.1\times10^{-3},2.1\times10^{-3},1.4\times10^{-3},7.2\times10^{-4},1.3\times10^{-4},4.5\times10^{-5}$ in (b), where we used the values of diffusion constant $D=0.1$, 0.05, 0.01, 0.005, 0.001, 0.0005 and the Lamb-Dicke parameter $\eta=0.25$, 0.125, 0.0625, 0.03125.

These two conditions can be cast in $D \gtrsim (K\eta^4)^{2/3} \gg \eta^4$, which is always attainable in the semiclassical regime ($\eta \ll 1$), independent of the value of D.

The approximation of the quantum propagator [Eq. (17)] allows us to write the Wigner function immediately before the kick n as

$$\tilde{W}_n(\mathbf{x}) = \tilde{W}_n^{\mathrm{cl}}(\mathbf{x}) + \chi \sum_{j=0}^{n} \tilde{G}_j(\mathbf{x}) + \mathcal{O}(\chi^2), \tag{18}$$

where the tilde indicates the action of the purely diffusive reservoir and we define the phase space function,

$$\tilde{G}_j(\mathbf{x}) = \int d\mathbf{x}_n \tilde{L}^{\mathrm{cl}}(\mathbf{x}^R,\mathbf{x}_n)$$

$$\vdots$$

$$\times \int d\mathbf{x}_j \sin(q_j) f(y_j) \tilde{L}^{\mathrm{cl}}(\mathbf{x}_j^R,\mathbf{x}_{j-1})$$

$$\vdots$$

$$\times \int d\mathbf{x}_0 \tilde{L}^{\mathrm{cl}}(\mathbf{x}_1^R,\mathbf{x}_0) W_0(\mathbf{x}_0). \tag{19}$$

Equation (18) is obtained by iterating the evolution given by Eq. (5) with the smoothed Wigner propagator in Eq. (17) from the initial condition $W_0(\mathbf{x}_0)$, and keeping only terms of first order in χ. Hence, when $\chi \ll 1$, for the separation between the classical and quantum distributions, we obtain

$$\mathcal{D}_n \approx \chi \int d\mathbf{x} \left| \sum_{j=0}^{n} \tilde{G}_j(\mathbf{x}) \right|. \tag{20}$$

The scaling law proportional to χ, obtained in Eq. (20), is confirmed in Fig. 6 where the exact numerical calculation of $\mathcal{D}_n/\chi$ as a function of the number of kicks n for $K=0.5$ and $K=1.5$ and a wide range of values of η and D are displayed. It is noticed that for values of χ which are order of magnitude different, all the curves $\mathcal{D}_n/\chi$ versus n fit in the same scale. So, independent of the value of D, in the semiclassical limit we have $D \gg (K\eta^4)^{2/3} \gg \eta^4$, and thus the separation between the quantum and the classical distributions decreases with η^4, becoming arbitrarily small. The curves in Fig. 6 were generated for an initial coherent state whose Gaussian Wigner function, $W_0(\mathbf{x}_0)$, is centered in the phase space point, $\mathbf{x}_0=(0,1.1)$ (Fig. 1). However we get similar results when $W_0(\mathbf{x}_0)$ is centered at $\mathbf{x}_0=(0.7,0)$. It is worth remembering that the initial distributions considered explore regions of phase space with essentially regular classical dynamics when K=0.5, while for K=1.5 these regions correspond to a mixed classical dynamics. We also obtained similar results when we considered the case with $K=1$.

The range of values of χ for which the scaling law in Eq. (20) works is shown in Fig. 7 where we plot the first peak of $\mathcal{D}_n$, corresponds to the maximum separation between the classical and the quantum distributions, as a function of χ. We clearly see that the proportionality of $\mathcal{D}_n$ with χ is, in general, valid for $\chi<1$ with a slight dependence with the position in phase space of the initial distribution [comparing plot (a) and (b)]. We can also observe that when the phase space regions explored by the initial distribution are regular or mixed, the proportionality is valid up to values $\mathcal{D}_n<1$, but, if the regions explored are essentially chaotic, the proportionality with χ is valid up to $\mathcal{D}_n \approx 1$ (see inset of Fig. 7).

Also, it is interesting to compare the behavior of the time position of the first peak of $\mathcal{D}_n$ as a function of η of our curves with its behavior when $K=2$ found in Ref. [15]. In that case the initial distribution was centered at the origin of phase space, that for $K=2$ it is an hyperbolic fixed point surrounded by a chaotic region [Fig. 1(d)]. The time position of the peak occurred approximately for $n_{\mathrm{peak}}(\eta) \approx (1/\Lambda)\ln(1/\eta)$, where Λ is the expansion eigenvalue of the linear map at the origin. However, in our case the time position of the first peak of $\mathcal{D}_n$ is almost the same for all values of η. We need to realize that the first peak of $\mathcal{D}_n$ signals the

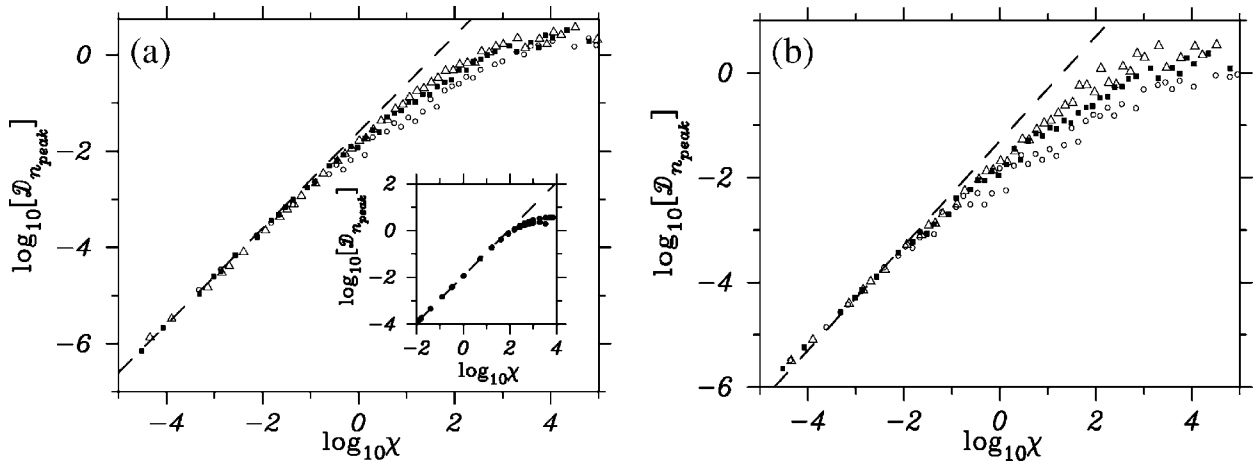

FIG. 7. The maximum distance between quantum and classical distributions given by the value of the first peak of $\mathcal{D}_n$ at $n=n_{\text{peak}}$ as a function of χ. The initial distribution is centered at $\mathbf{x}_0=(0,1.1)$ in (a) and $\mathbf{x}_0=(0.7,0)$ in (b). The marks (○) are for $K=0.5$, the (■) for $K=1.0$, and (△) for $K=1.5$. The region of linear behavior of $\mathcal{D}_{n_{\text{peak}}}$ as a function of χ is highlighted by the dashed line with a unit value of the slope. The inset is borrowed from Ref. [15] when the initial distribution explores a chaotic region in phase space of the classic KHO. We use the value of the Lamb-Dicke parameters $\eta=0.5,0.25,0.125,0.0625,0.03125$, and the diffusion constant $D=5\times10^{-6},1\times10^{-5},5\times10^{-5},1\times10^{-4},5\times10^{-4},1\times10^{-3},5\times10^{-3},1\times10^{-2},5\times10^{-2},10^{-1}$.

moment when the decoherence effects start to dominate, restraining the separation of the classical and quantum distributions produced by the presence of nonlinearities in the system. When the underlying classical dynamics are chaotic, these nonlinearities are reached in a very short time so the diffusion dominates when these nonlinearities have already been reached. This is reflected in the behavior of the position of the peak, which is a memory of the behavior of the separation time Eq. (10) without the action of a reservoir. Conversely, when the underlying classical dynamics are regular or mixed, the time to reach the nonlinearities is very slow so almost immediately the diffusion washed out any memory (in the position of peak) of the separation time in Eq. (11).

Our exact numerical simulations together with those in Ref. [15] confirm the validity of the scale-law obtained in Eq. (20) that rules the quantum to classical transition of the KHO in the semiclassical regime and in the presence of decoherence, independent of the underlying classical behavior. Furthermore, the exact numerical calculations suggest that the approximation in Eq. (18) that leads to Eq. (20) must be correct. Therefore, the same scale-law proportional to χ is valid for the mean values of any smooth observables throughout the evolution of the system. Indeed, the mean value of an observable $\hat{O}$ in a state represented by the Wigner function $W(\mathbf{x})$ is given by

$$\langle\hat{O}\rangle = \int d\mathbf{x} O(\mathbf{x}) W(\mathbf{x}), \tag{21}$$

where $O(\mathbf{x})$ is the Weyl symbol of $\hat{O}$ obtained through the Weyl transform in Eq. (4) replacing $\hat{\rho}/4\pi\eta^2 \to \hat{O}$ [3]. The classical mean value is obtained in the same way, substituting $O(\mathbf{x})$ by the classical function $O^{\text{cl}}(\mathbf{x})$ and $W(\mathbf{x})$ by the classical distribution $W^{\text{cl}}(\mathbf{x})$. So, for every smooth operator in the semiclassical regime, we can take $O(\mathbf{x}) \approx O^{\text{cl}}(\mathbf{x})$ [26] and in the presence of decoherence, we use the result in Eq. (18) to get

$$\langle\hat{O}\rangle_n - \langle\hat{O}\rangle_n^{\text{cl}} = \chi \int d\mathbf{x} O_n^{\text{cl}}(\mathbf{x}) \sum_{j=0}^{n} \tilde{G}_j(\mathbf{x}) + \mathcal{O}(\chi^2). \tag{22}$$

V. FINAL REMARKS

We have studied the effect of decoherence in the quantum-classical transition of the KHO when the classical dynamics is regular or mixed (with small regions of chaotic behavior). Our approach was based on the behavior of the distance $\mathcal{D}_n$ [Eq. (12)] as a function of time. We have shown that, without the presence of a reservoir, $\mathcal{D}_n$ clearly indicates that the quantum unitary evolution separates from the classical evolution because it reaches values that do not decrease in the classical limit. When the initial distribution explores regions of regular classical dynamics, the separation time t_s scales as a power law with the effective Planck constant, that is, $t_s \approx \tau/\hbar_{\text{eff}}^{\alpha}$. We have observed that when the degree of mixing increases, this power-law is no longer valid.

When the system is in contact with a purely diffusive reservoir, we have extended the results of Ref. [15] for regular and mixed classical dynamics showing that also in these regimes $\mathcal{D}_n$ is proportional to $\chi=K\hbar_{\text{eff}}^2/4D^{3/2}$ when $\chi<1$. This implies that in the semiclassical regime ($\hbar_{\text{eff}} \ll 1$) and, independent of the values of the diffusion constant D or the classical dynamics explored by the initial distribution, the quantum-classical difference $\mathcal{D}_n$ goes to zero as $\hbar_{\text{eff}}^2$. The conditions for the proportionality between $\mathcal{D}_n$ and χ can be condensed in the inequality $D \gg (K\hbar_{\text{eff}}^2)^{2/3} \gg \hbar_{\text{eff}}^2$. This is the relation of the strength of noise and the semiclassical parameter for the KHO in order to obtain the classical limit for all the regimes of its underlying classical dynamics correctly. We would like to remark that because of the smallness of $\mathcal{D}_n$, in the semiclassical regime, the concept of separation time is no longer meaningful.

Finally, our results and those from Ref. [15] indicate that the conjecture presented in Ref. [16] may be extended, in general, for all types of classical dynamics. However, it seems that χ should enter a parameter that controls the degree of mixing of the considered system and not directly the Lyapunov coefficient that characterizes the exponential divergence of trajectories in fully chaotic classical systems.

Comparing our result for the KHO and the one in Ref. [16] for the noisy cat map, we could see that the power of the coupling to the environment D entering in the definition of parameter χ depends on the particular system considered. It will be the aim of future works to test the genericity of our findings in other systems.

ACKNOWLEDGMENTS

We acknowledge Luiz Davidovich for fruitful comments. D.A.W. gratefully acknowledges support from CONICET (Argentina) and PROSUL (Brazil). F.T. acknowledges the hospitality at the "Departamento de Física "J. J. Giambiagi"," FCEN, UBA, where this work started.

[1] L. E. Ballentine, Yumin Yang, and J. P. Zibin, Phys. Rev. A **50**, 2854 (1994).
[2] E. Wigner, Phys. Rev. **40**, 749 (1932).
[3] M. Hillery, R. F. O'Connell, M. O. Scully, and E. P. Wigner, Phys. Rep. **106**, 121 (1984).
[4] G. P. Berman and G. M. Zaslavsky, Physica A **91**, 450 (1978).
[5] M. V. Berry, N. L. Balazs, M. Tabor, and A. Voros, Ann. Phys. (N.Y.) **122**, 26 (1979).
[6] B. V. Chirikov, F. M. Izrailev, and D. L. Shepelyansky, Physica D **33**, 77 (1988).
[7] G. P. Berman, V. Yu Rubaev, and G. M. Zaslavsky, Nonlinearity **4**, 543 (1991).
[8] Z. P. Karkuszewski, J. Zakrzewski, and W. H. Zurek, Phys. Rev. A **65**, 042113 (2002).
[9] A. R. R. Carvalho, R. L. de Matos Filho, and L. Davidovich, Phys. Rev. E **70**, 026211 (2004).
[10] L. Davidovich, F. Toscano, and R. L. de Matos Filho, "*Decoherence and the Quantum-Classical Transition in Phase Space*," in *AIP Conference Proceedings, Atomic Physics 19: XIX International Conference on Atomic Physics-ICAP 2004*, edited by L. G. Marcassa, K. Helmerson, and V. S. Bagnato (2005), Vol. 770, pp. 301–310; L. Davidovich, F. Toscano, and R. L. de Matos Filho, "*Decoherence and the Quantum-Classical Limit in Phase Space*," in *Proceedings of SPIE—The International Society for Optical Engineering*, Vol. 5842, edited by P. R. Hemmer, J. R. Gea-Banacloche, P. Heszler Sr., and M. S. Zubairy, (2005), pp. 220–231.
[11] W. H. Zurek and J. P. Paz, in "*Numerical Exploration of Hamiltonian Systems*," *Proceedings of Les Houches* (1981), session XXXVI (North Holland, 1983), Sec. 7, p. 136; W. H. Zurek, Phys. Scr., T **76**, 186 (1998); M. Berry, in *Quantum Mechanics: Scientific Perspectives on Divine Action*, edited by K. W.-M. R. J. Russell, P. Clayton, and J. Polkinghorne (Vatican Observatory-CTNS Publications, Berkeley, 2001), p. 4154.
[12] W. H. Zurek and J. P. Paz, Phys. Rev. Lett. **72**, 2508 (1994).
[13] W. H. Zurek, Rev. Mod. Phys. **75**, 715 (2003).
[14] I. Garcia-Mata and M. Saraceno, Mod. Phys. Lett. B **19**, 341 (2005).
[15] F. Toscano, R. L. de Matos Filho, and L. Davidovich, Phys. Rev. A **71**, 010101(R) (2005).
[16] A. K. Pattanayak, B. Sundaram, and Benjamin D. Greenbaum, Phys. Rev. Lett. **90**, 014103 (2003).
[17] S. A. Gardiner, J. I. Cirac, and P. Zoller, Phys. Rev. Lett. **79**, 4790 (1997).
[18] D. J. Wineland, C. Monroe, W. M. Itano, D. Leibfried, B. E. King, and D. M. Meekhof, J. Res. Natl. Inst. Stand. Technol. **103**, 259 (1998).
[19] J. Bertrand and P. Bertrand, Found. Phys. **17**, 397 (1987).
[20] L. G. Lutterbach and L. Davidovich, Phys. Rev. Lett. **78**, 2547 (1997); P. Bertet, A. Auffeves, P. Maioli, S. Osnaghi, T. Meunier, M. Brune, J. M. Raimond, and S. Haroche, Phys. Rev. Lett. **89**, 200402 (2002); F. de Melo, L. Aolita, F. Toscano, and L. Davidovich, Phys. Rev. A **73**, 030303 (2006).
[21] H. J. Korsch and M. V. Berry, Physica D **3**, 627 (1981).
[22] R. L. Hudson, Rev. Mod. Phys. **6**, 249 (1974).
[23] J. E. Moyal, Proc. Cambridge Philos. Soc. **45**, 99 (1949).
[24] D. Monteoliva and J. P. Paz, Phys. Rev. E **64**, 056238 (2001).
[25] M. Henon, "*Numerical Exploration of Hamiltonian Systems*," *Proceedings of Les Houches* (1981), Session XXXVI (North Holland, 1983), Sec. 7, p. 136.
[26] A. M. Ozorio de Almeida, Phys. Rep. **295**, 265 (1998).